https://doi.org/10.1093/plphys/kiac241 PLANT PHYSIOLOGY 2022: 189: 2193–2209

Plant Physiology®

Research Article

SKI-INTERACTING PROTEIN interacts with SHOOT MERISTEMLESS to regulate shoot apical meristem formation

Ruiqi Li [1,2], Zhifeng Wei [2], Yan Li [2], Xudong Shang [2], Ying Cao [2], Liusheng Duan [1] and Ligeng Ma [2,*,†]

1 State Key Laboratory of Plant Physiology and Biochemistry, College of Agriculture and Biotechnology, China Agricultural University, Beijing 100193, China
2 College of Life Sciences, Capital Normal University, Beijing 100048, China

*Author for correspondence: ligeng.ma@cnu.edu.cn
†Senior author

R.L., Y.C., L.D., and L.M. designed the concept. R.L., Z.W., Y.L., and X.S. did the experimental work. Y.C. and L.D. supervised parts of this project. R.L. and L.M. wrote the manuscript with input from all the authors.
The author responsible for distribution of materials integral to the findings presented in this article in accordance with the policy described in the Instructions for Authors (https://academic.oup.com/plphys/pages/general-instructions) is: Ligeng Ma (ligeng.ma@cnu.edu.cn).

Abstract

The shoot apical meristem (SAM), which is formed during embryogenesis, generates leaves, stems, and floral organs during the plant life cycle. SAM development is controlled by SHOOT MERISTEMLESS (STM), a conserved Class I KNOX transcription factor that interacts with another subclass homeodomain protein, BELL, to form a heterodimer, which regulates gene expression at the transcriptional level in Arabidopsis (*Arabidopsis thaliana*). Meanwhile, SKI-INTERACTING PROTEIN (SKIP), a conserved protein in eukaryotes, works as both a splicing factor and as a transcriptional regulator in plants to control gene expression at the transcriptional and posttranscriptional levels by interacting with distinct partners. Here, we show that, similar to plants with a loss of function of *STM*, a loss of function of *SKIP* or the specific knockout of *SKIP* in the SAM region resulted in failed SAM development and the inability of the mutants to complete their life cycle. In comparison, Arabidopsis mutants that expressed *SKIP* specifically in the SAM region formed a normal SAM and were able to generate a shoot system, including leaves and floral organs. Further analysis confirmed that SKIP interacts with STM in planta and that SKIP and STM regulate the expression of a similar set of genes by binding to their promoters. In addition, STM also interacts with EARLY FLOWERING 7 (ELF7), a component of Polymerase-Associated Factor 1 complex, and mutation in *ELF7* exhibits similar SAM defects to that of *STM* and *SKIP*. This work identifies a component of the STM transcriptional complex and reveals the mechanism underlying SKIP-mediated SAM formation in Arabidopsis.

Introduction

The aerial tissues and organs of angiosperms, including leaves, stems, and flowers, are initiated through the activity of the shoot apical meristem (SAM), which generates organs in a predictable and regular pattern (Scheres, 2007; Dinneny and Benfey, 2008). The SAM is a highly organized group of cells that can be divided into distinct zones with different functions (Hake et al., 2004; Scheres, 2007). These functional zones include the central zone (CZ), which contains a pool of slowly dividing pluripotent stem cells called the stem cell

Received March 01, 2022. Accepted May 02, 2022. Advance access publication May 28, 2022

niche; the peripheral zone (PZ), which surrounds the CZ and in which cells divide rapidly to generate leaf primordia; and the rib zone, which lies below the CZ and contains cells that divide to form stems (Scheres, 2007; Dinneny and Benfey, 2008). Apart from this functional classification, the SAM is organized into three clonally distinct layers of cells. The cells in the outermost L1 layer and the subepidermal L2 layer divide in an anticlinal manner, while the underlying corpus forms a multilayered structure in which cells divide in random orientations (Weigel and Jurgens, 2002). Therefore, SAM formation in angiosperms requires a precise balance in cell division patterns among cells that belong to distinct zones and clonal layers (Williams, 2021).

The organization of these distinct zones and cell layers is maintained by the mobile homeodomain protein SHOOT MERISTEMLESS (STM) in Arabidopsis (*Arabidopsis thaliana*) (Long et al., 1996; Tsuda and Hake, 2015). STM is a Class I KNOX transcription factor, part of a small family of three amino acid loop extension (TALE) homeobox proteins. There are four Class I members in Arabidopsis: STM, Knotted-1-like 1 (KNAT1), also called BREVIPEDICELLUS, KNAT2, and KNAT6 (Hake et al., 2004; Hay and Tsiantis, 2010). They share similar expression patterns and are broadly expressed in the SAM with enrichment in certain regions, including the organ boundary. Nevertheless, STM plays a dominant role in maintaining SAM activity (Long et al., 1996). Repression of *STM* expression outside of the SAM is important for lateral organ formation, and is redundantly controlled by ASYMMETRIC LEAVES 1 (AS1), AS2, POLYCOMB REPRESSIVE COMPLEX 1 (PRC1)/PRC2, YABBY, and the phytohormone auxin (Byrne et al., 2000; Kumaran et al., 2002; Guo et al., 2008; Xu and Shen, 2008; Chung et al., 2019). A defect in *STM* expression within the SAM region or ectopic expression of *STM* outside of the SAM region causes defects in SAM formation and in the determination of cell fate and organ shape (Hake et al., 2004). STM is also required for axillary meristem initiation and branching in plants (Long and Barton, 2000; Shi et al., 2016; Zhang et al., 2018; Cao et al., 2020).

STM interacts with several members of another subclass of TALE homeodomain proteins called BELL family proteins to form heterodimers that activate or repress the expression of target genes at the transcriptional level (Cole et al., 2006; Hay and Tsiantis, 2010). STM activity can be controlled by regulating the translocation of STM from the nucleus to the cytosol (i.e. altering its accumulation in the nucleus) or by regulating the intercellular trafficking of STM, which alters its availability for protein–protein interactions (Balkunde et al., 2017). Several STM-interacting proteins that are required for the translocation of STM from the nucleus to the cytosol and for the intercellular trafficking of STM have been identified. They include BELL, which mediates STM nuclear import through the formation of a STM–BELL heterodimer (Cole et al., 2006); OVATE FAMILY PROTEIN and CHROMOSOMAL REGION MAINTENANCE 1, which are required for the transportation of STM from the nucleus to the cytosol (Hackbusch et al., 2005; Rutjens et al., 2009); FT INTERACTING PROTEIN (FTIP)3 and FTIP4, which are responsible for translocating STM from the plasma membrane to the nucleus by protecting STM from binding to the plasma membrane (Liu et al., 2018); and the microtubule-associated protein MOVEMENT PROTEIN 30 BINDING PROTEIN 2C and poly (ADP-ribose) polymerase domain-containing protein TWISTED-LEAF 1, which mediate the intercellular trafficking of STM via plasmodesmata (Winter et al., 2007; Xu et al., 2011; Cui et al., 2019). Thus, STM is a mobile transcription factor that regulates the expression of genes required for SAM formation and whose activity is regulated by its interacting partner proteins.

SKI-INTERACTING PROTEIN (SKIP) is a conserved protein from yeast to plants and metazoa (Folk et al., 2004; Wang et al., 2012). It is a component of the spliceosome and is required for the alternative splicing of pre-mRNAs in yeast and human cells (Wahl et al., 2009; Wan et al., 2020). In plants, SKIP works as a bifunctional factor (i.e. a splicing factor and a transcriptional regulator) to regulate gene expression at both the transcriptional and posttranscriptional levels (Cao and Ma, 2019). It integrates into the spliceosome by interacting with components of the spliceosome, including MOS4-Associated Complex 3 (MAC3) (Palma et al., 2007; Li et al., 2019), Spliceosomal Timekeeper Locus 1 (STIPL1) (Jones et al., 2012; Li et al., 2019), and Pleiotropic Regulatory Locus 1 (PRL1) (Németh et al., 1998; Li et al., 2019). SKIP plays an essential regulatory role in the circadian clock and salt stress responses in Arabidopsis by controlling alternative pre-mRNA splicing (Wang et al., 2012; Feng et al., 2015; Li et al., 2019). Further, SKIP interacts with a transcriptional activation complex, Polymerase-Associated Factor 1 complex (Paf1c), which mediates flowering through the activation of *FLOWERING LOCUS C* (*FLC*) transcription (Cao et al., 2015; Li et al., 2019). Interestingly, other spliceosome components, including MAC3, STIPL1, and PRL1, are not required for the regulation of *FLC* expression and flowering, and Paf1c is not required for the regulation of salt responses (Li et al., 2019). Therefore, SKIP integrates into two distinct complexes to mediate the floral transition and stress responses at the transcriptional and posttranscriptional levels of gene expression, respectively, in Arabidopsis (Li et al., 2019). However, Paf1c is a mediator of histone monoubiquitination and methylation during transcription in eukaryotes from humans to plants (Zhu et al., 2005; Cao et al., 2015), and SKIP is a transcriptional coregulator of SKIP-mediated transcription. Thus, SKIP requires a partner to achieve target selection during SKIP-mediated gene expression. However, no specific transcription factor or other class of DNA-binding protein that interacts with SKIP to regulate the expression of target genes in plants has been identified.

In this study, we uncovered a direct interaction between SKIP and STM in planta, and we verified that both SKIP and STM bind to the promoters of genes required for SAM

formation and that this binding is required for the transcription of those genes and SAM formation. Our findings not only indicate an additional function for SKIP, they also reveal both a transcription factor that works with SKIP and a STM-interacting protein that regulates SAM development in Arabidopsis.

Results

The mutation of *SKIP* produces a defect in SAM formation

Previously, we isolated a mutant, *skip-1*, which carries a 22-nucleotide deletion in *SKIP* that results in a frameshift, which is predicted to generate a truncated protein (Wang et al., 2012). The *skip-1* mutant exhibits early flowering with a long-period clock phenotype (Wang et al., 2012; Cao et al., 2015). However, when we characterized a *SKIP* T-DNA insertion mutant, *skip-2*, it exhibited severe dwarfism, infertility, and strong developmental defects that prevented it from completing its life cycle (Figure 1, A–C and Supplemental Figure S1, A–C). The transformation of *SKIP* genomic DNA (with a GFP tag) into *skip-2* plants fully complemented all of the developmental defects observed in *skip-2*, from the seedling stage to the adult stage (Figure 1, A–E), suggesting that the defects observed in *skip-2* were due to the mutation of *SKIP*. Further analysis revealed that *skip-1* plants expressed a truncated version of SKIP while no SKIP protein was detected in *skip-2* (Figure 1F); thus, *skip-1* represents a weak allele, while *skip-2* is a strong allele.

Given that *skip-2* plants exhibited severe developmental defects (Figure 1, A–E) and that postembryonic development in plants is directed by the SAM, we studied SAM development in wild-type and *skip-2* plants. Wild-type plants produced a normal SAM and generated leaves, shoots, and floral organs during their life cycle, but no clear SAM was observed in *skip-2*, and no normal leaves or shoots were generated (Figure 2A). At the cellular level, the SAM in wild-type plants exhibited a clear cellular organization, with L1, L2, and L3 cells, while the enlarged cells in the SAM of *skip-2* plants were not organized and no clear L1, L2, or L3 cells were observed (Figure 2, B and C). Notably, the transformation of *SKIP* genomic DNA into *skip-2* plants fully complemented all of the SAM defects observed in the original mutant (Figure 2, A–C). Further analysis suggested that SAM size is decreased in both *skip-1* and *skip-2* compared with that of wild-type plants in terms of width, height and area, *skip-2* exhibited stronger phenotype than *skip-1*, and this decrease in SAM size was rescued in the complementation line (Figure 2, D–F). Those result indicated that *skip-1* plants exhibited a mild defect in the SAM compared with wild-type and *skip-2* plants (Figure 2, A–F), consistent with their semi-dwarf phenotype (Supplemental Figure S2). Together, these results suggest that SKIP is required for SAM formation and maintenance, and that the mutation of *SKIP* causes a defect in SAM formation.

The truncated SKIP protein in *skip-1* is partly functional

The *skip-1* mutants expressed a truncated SKIP protein and exhibited a weaker SAM phenotype than did *skip-2* plants (Figures 1F and 2, A–F); thus, the truncated SKIP protein was partly functional in terms of SAM formation. SKIP contains three domains: N-terminal, SNW, and C-terminal domains (Li et al., 2016). To determine the domain requirement for the function of SKIP in SAM formation in Arabidopsis, we expressed different domains of SKIP in *skip-2* plants driven by the native *SKIP* promoter. Transformation of the SNW ($SKIP_S$), C-terminal ($SKIP_C$), N-terminal + SNW ($SKIP_{NS}$), or SNW + C-terminal ($SKIP_{SC}$), but not the N-terminal ($SKIP_N$), domain rescued the phenotypes of the *skip-2* mutant at least partly in terms of SAM formation and development (Figure 3, A and B), root length (Figure 3C), fresh weight (Figure 3D), rosette leaf number (Figure 3E), and leaf emergence rate (Figure 3F) compared with the transformation of full-length SKIP, which completely rescued the defects observed in *skip-2*. Among these truncated proteins, which contained various SKIP domains, $SKIP_{NS}$ and $SKIP_{SC}$ were more effective at rescuing the *skip-2* mutant phenotypes compared with $SKIP_S$, $SKIP_S$ was more effective than $SKIP_C$, and $SKIP_N$ was not functional in Arabidopsis (Figure 3, A–F). These results demonstrate that the truncated SKIP proteins were at least partially functional in *skip-2* in terms of SAM formation and maintenance, suggesting that SKIP functions in a domain-friendly and flexible manner in Arabidopsis.

SKIP interacts with STM in Arabidopsis

SKIP works both as a splicing factor and a transcriptional coregulator in plants (Wang et al., 2012; Cao et al., 2015). To understand how SKIP regulates SAM formation, we performed a yeast two-hybrid screen with an Arabidopsis yeast two-hybrid library to identify SKIP-interacting proteins. Among the more than 10 million clones examined, STM, a homeodomain transcription factor that is required for SAM formation in Arabidopsis (Long et al., 1996), was identified as a SKIP-interacting protein. This observation was confirmed in a separate yeast two-hybrid assay using SKIP and STM (Figure 4A). Each of the three domains of SKIP (N-terminal, SNW, and C-terminal domains) was capable of interacting with full-length STM, although the strength of the interaction was weaker than that using full-length SKIP or the N-terminal + SNW ($SKIP_{NS}$) or SNW + C-terminal ($SKIP_{SC}$) domains of SKIP, and the interaction between the SKIP C-terminal domain ($SKIP_C$) and STM was the weakest one among them (Supplemental Figure S3, A and B). The interaction between full-length or truncated SKIP (except $SKIP_N$) and STM is consistent with the function of full-length or truncated SKIP in rescuing the defects observed in *skip-2* plants (Figure 3, A–F). As for $SKIP_N$, although it interacted with STM in yeast (Supplemental Figure S3, A and B), it did not localize to the nucleus and was observed instead in the cytosol (Li et al., 2016). Since SKIP functions in the

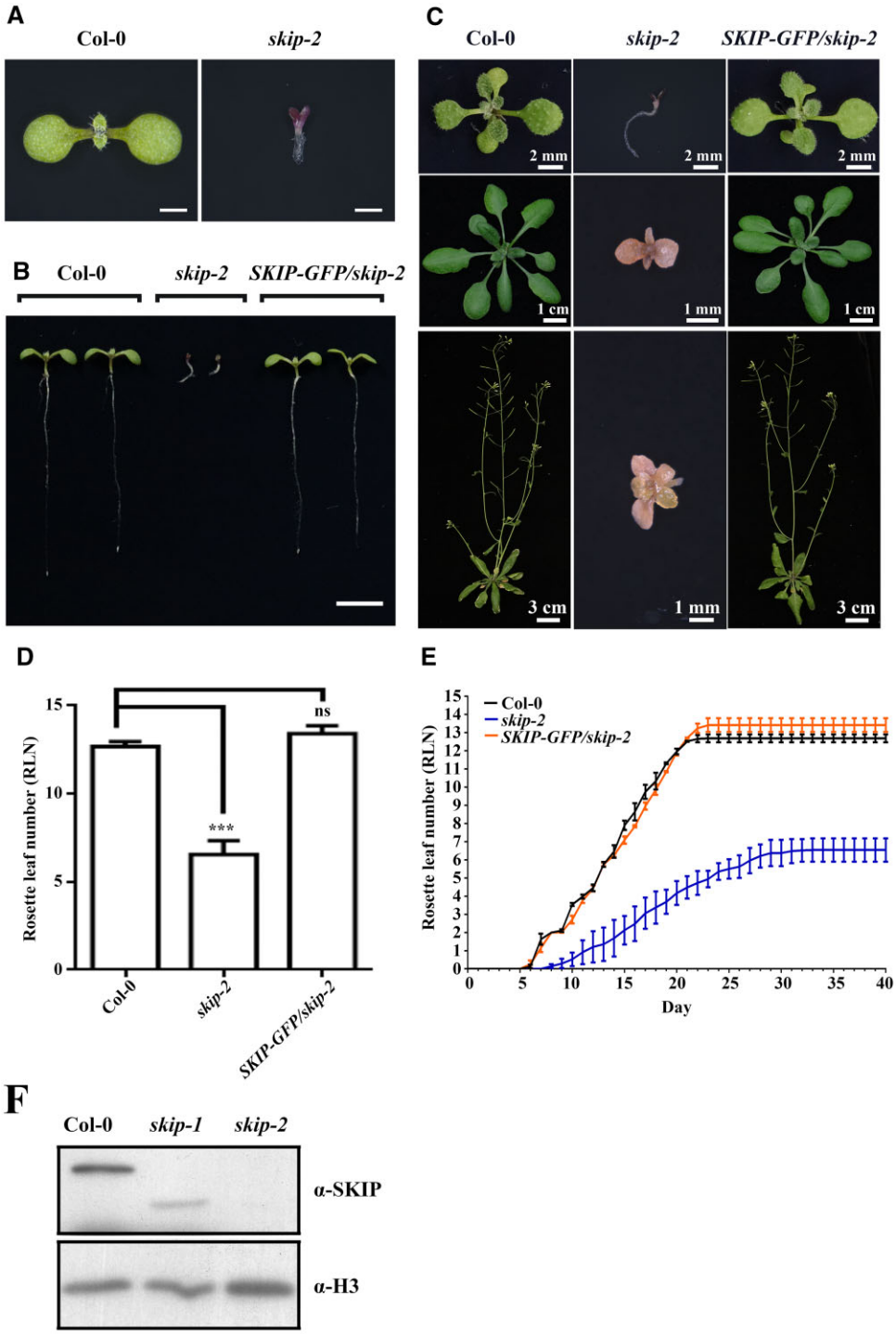

Figure 1 SKIP is an essential part of the Arabidopsis life cycle. A, Seven-day-old wild-type and *skip-2* plants. Scale bar = 1 mm. B, Seven-day-old wild-type, *skip-2*, and *skip-2* complemented (*pSKIP::SKIP-GFP/skip-2*) plants. At least 10 independent transgenic lines with similar phenotypes were observed; one representative line is shown. Scale bar: 1 cm. C, Wild-type, *skip-2*, and *skip-2* complemented (*pSKIP::SKIP-GFP/skip-2*) plants at 14 days old (top), 21 days old (middle), and 35 days old (bottom). D, The rosette leaf number in wild-type, *skip-2*, and *skip-2* complemented (*pSKIP::SKIP-GFP/skip-2*) plants. The data represent the mean ± SD from three biological replicates. ***$P < 0.001$ (Student's *t* test). ns: no significant difference. E, Leaf emergence in wild-type, *skip-2*, and *skip-2* complemented (*pSKIP::SKIP-GFP/skip-2*) plants. The data represent the mean ± SD from three biological replicates. F, Western blot analysis of SKIP protein expression from wild-type and *skip* alleles using anti-SKIP antibodies.

nucleus, it is not surprising that $SKIP_N$ was not functional in Arabidopsis.

Further analysis indicated that SKIP and STM were colocalized in nuclear speckles (Figure 4B), and a strong fluorescence resonance energy transfer (FRET) emission signal was detected in the nuclear speckles of cells coexpressing GFP-SKIP and STM-RFP; this observation was further confirmed in a photobleaching assay using *Nicotiana*

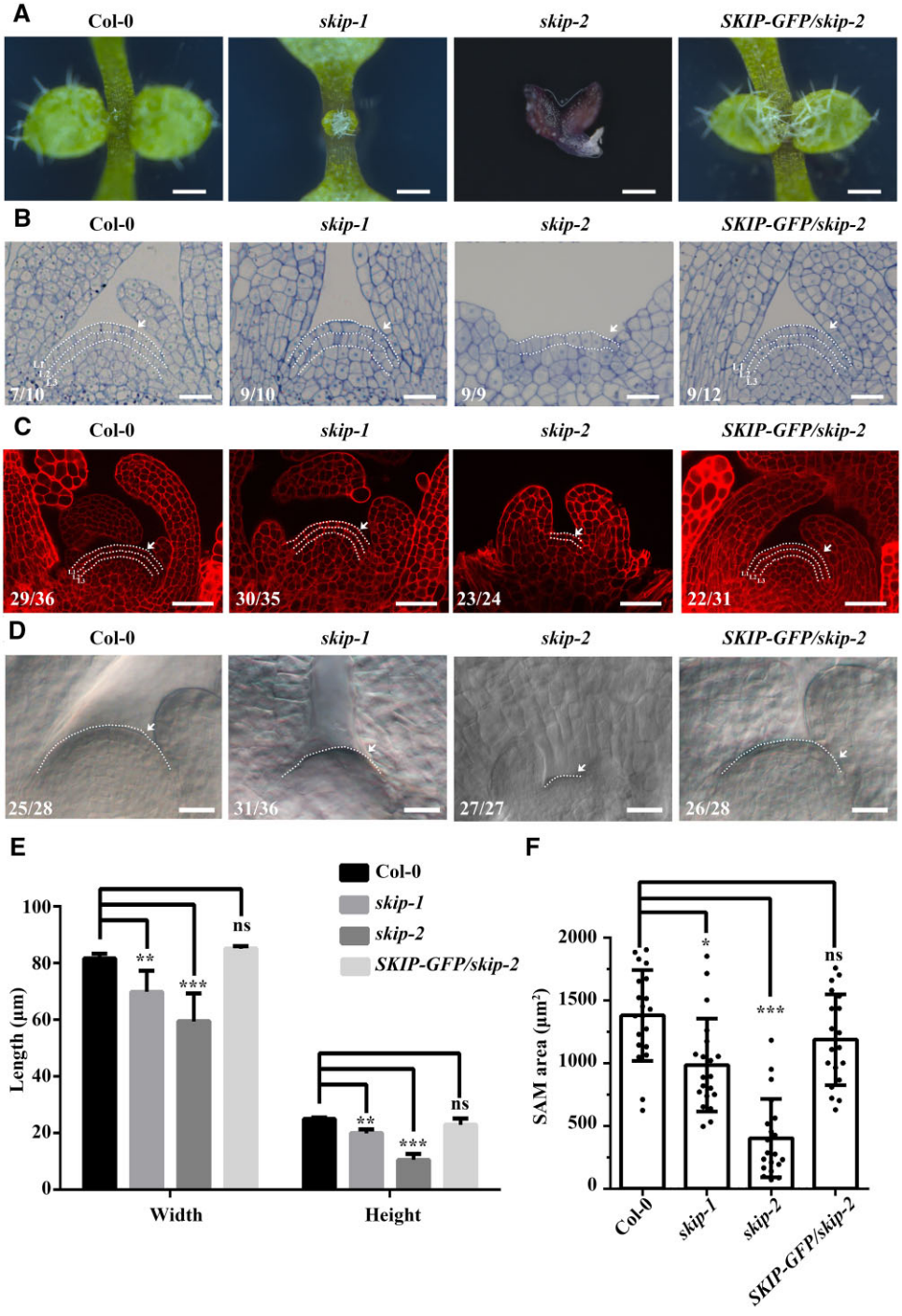

Figure 2 The mutation of *SKIP* confers SAM defects in Arabidopsis. In contrast to wild-type and *skip-2* complemented (*pSKIP::SKIP-GFP/skip-2*) plants, *skip-1* and *skip-2* exhibited defects in SAM development. A, Dissecting microscope images of the shoot apices of 7-day-old plants. Scale bar: 400 μm. B, Microscopic images of the SAM in 7-day-old plants stained with toluidine blue. Scale bar: 20 μm. C, Laser scanning confocal microscope observations of the SAM following mPS-PI staining. Scale bar: 40 μm. D, Differential interference contrast microscopy images of the SAM. Scale bar: 20 μm. White dashed lines in (B)–(D) mark the cell layers; arrows indicate the SAM. Numbers indicate the number of plants that exhibited a similar pattern out of the total number of plants observed. E, SAM width and height of the SAM measured shown in (C). The data represent the mean ± SD from 30 SAM. $^{**}P < 0.01$. $^{***}P < 0.001$ (Student's *t* test). F, SAM area measured shown in (D). The data represent the mean ± SD from 20 SAM. $^{*}P < 0.05$. $^{***}P < 0.001$ (Student's *t* test).

benthamiana cells (Figure 4, C and D). Although it was not as clear as in *N. benthamiana* cells, STM-VENUS localized in and co-localized with SKIP-CERULEAN in the nuclear speckles of SAM cells in Arabidopsis (Supplemental Figure S4). Finally, the interaction between SKIP and STM in Arabidopsis was confirmed in a co-immunoprecipitation

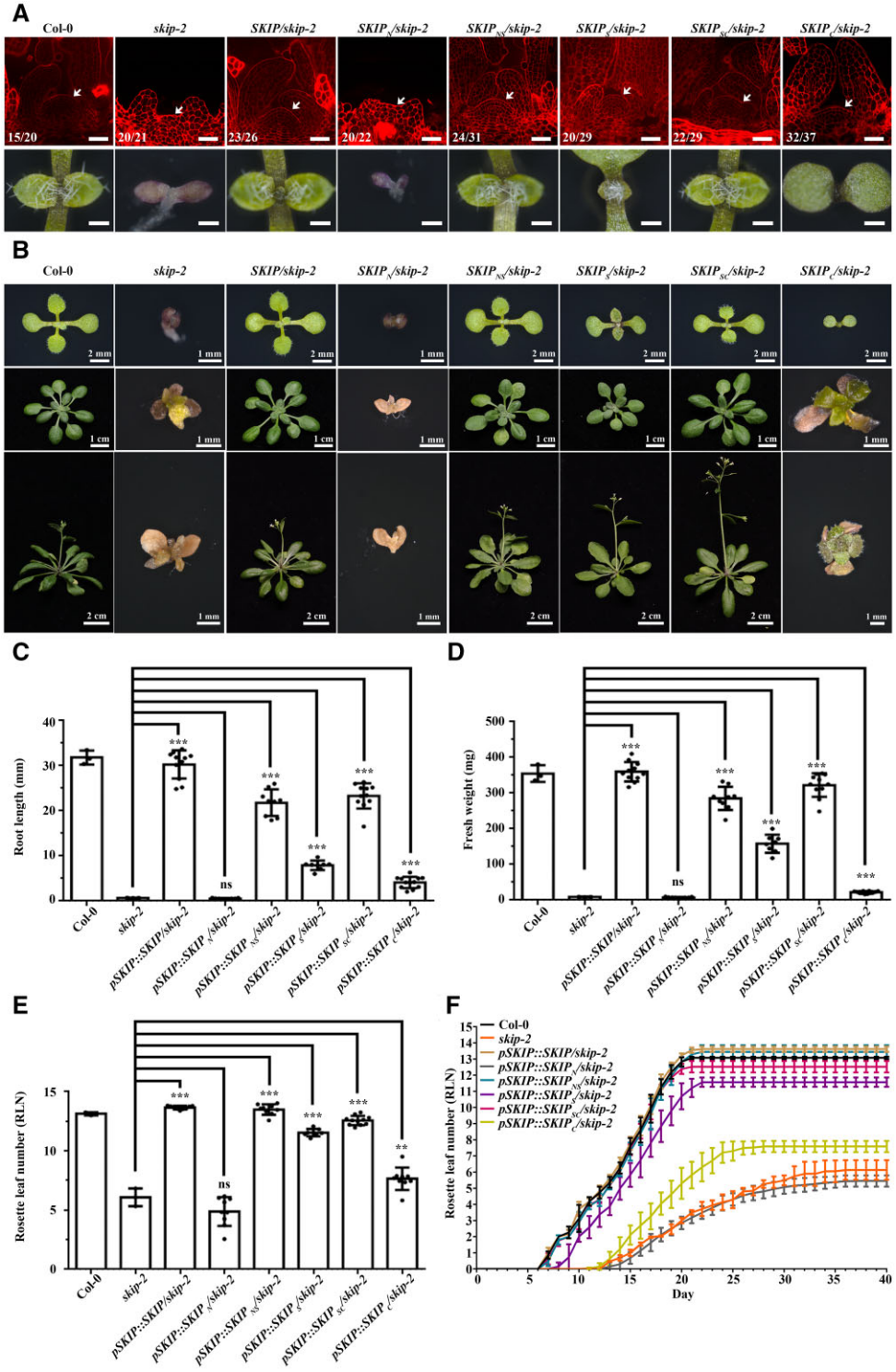

Figure 3 Truncated SKIP proteins were partially functional in Arabidopsis. A, Laser scanning confocal microscope observations of the SAM following mPS-PI staining (top). Scale bar: 40 μm. Arrows indicate the SAM. Numbers indicate the number of plants that exhibited a similar pattern out of the total number of plants observed. Dissecting microscope images of the shoot apices of 7-day-old plants (bottom). Scale bar: 400 μm. B, The development of wild-type, *skip-2*, and *skip-2* plants transformed with full-length or different truncated versions of *SKIP* at 10 days old (top), 21 days old (middle), and 28 days old (bottom). At least 10 independent transgenic lines exhibited a similar phenotype; one representative independent line for each is shown. C, The root length in wild-type, *skip-2*, and *skip-2* plants transformed with full-length or different truncated versions of *SKIP* at 7 days old. D, The fresh weight of wild-type, *skip-2*, and *skip-2* plants transformed with full-length or different truncated versions of *SKIP* at 14 days old. E, The rosette leaf number in wild-type, *skip-2*, and *skip-2* plants transformed with full-length or different truncated versions of *SKIP* at 28 days old. F, The emergence of leaves in wild-type, *skip-2*, and *skip-2* plants transformed with full-length or different truncated versions of *SKIP* at 40 days old. For the wild-type and *skip-2* plants in (C)–(F), the data represent the mean ± SD from three biological replicates. For each transgenic *SKIP* line in (C)–(F), the data represent the mean ± SD from 10 independent lines, and for each independent transgenic line, the data represent the mean from three biological replicates. $^{**}P < 0.01$. $^{***}P < 0.001$ (Student's *t* test).

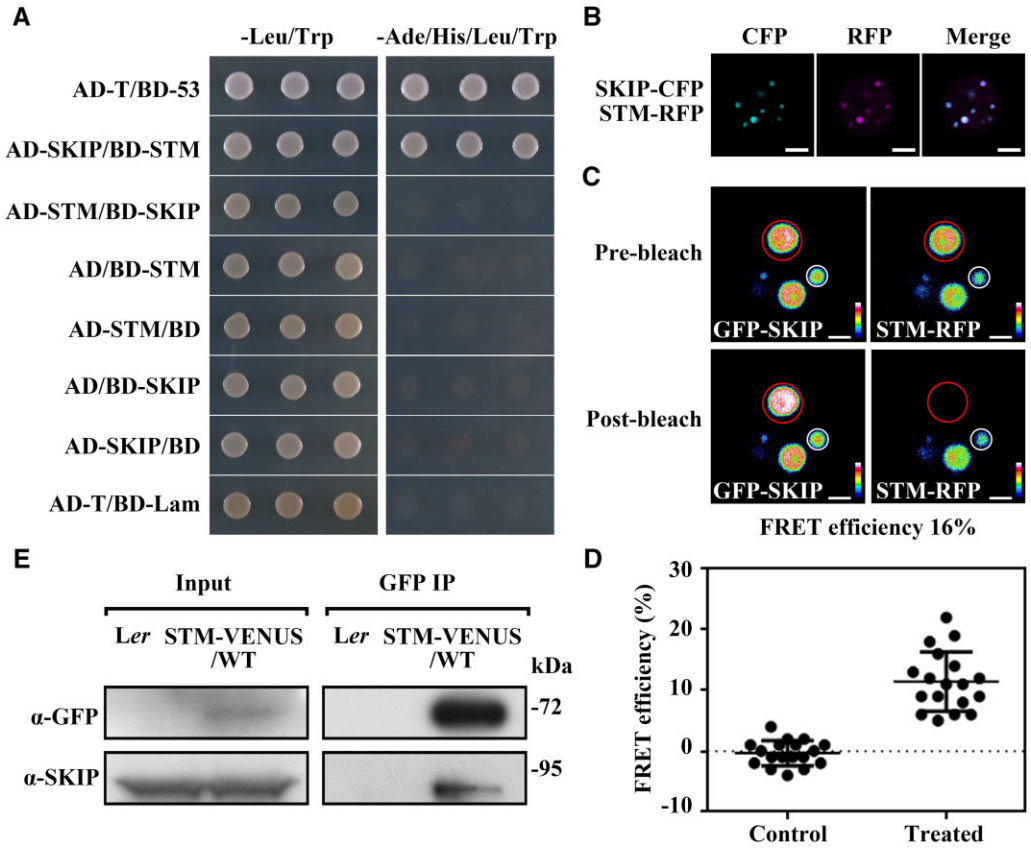

Figure 4 SKIP interacts physically with STM in planta. A, Yeast two-hybrid assay. AD-T/BD-53 is the positive control; AD-T/BD-Lam is the negative control. The interaction between SKIP and STM was assessed by growth on medium lacking leucine and tryptophan (−Leu/Trp, as a growth control) or lacking adenine, histidine, leucine, and tryptophan (−Ade/His/Leu/Trp, as a growth test). B, Colocalization assay in *N. benthamiana* cells. Laser scanning confocal microscope images from the CFP, RFP, and both (Merge) channels are shown. Scale bar: 5 μm. C, FRET assay in *N. benthamiana* cells. Laser scanning confocal microscope images from the GFP and RFP channels before and after SKIP-RFP photobleaching are shown. Different colors indicate the difference in fluorescence intensity in the barcode. Efficiency of FRET = (post ID-pre ID)/post ID, where ID is the intensity of the donor (GFP). Scale bar: 2 μm. D, The FRET efficiency from individual cells of three independent biological replicates. The control data were calculated from the nuclear speckle marked with a white circle in (C). The treated data were calculated from the nuclear speckle marked with a red circle in (C). The data represent the mean ± SD from 18 cells. E, Co-IP assay of the interaction between SKIP and STM in Arabidopsis. Total protein from inflorescences containing only unopened flowers in a wild-type (*Ler*) or *pSTM::STM-VENUS* (*Ler* background) background was immunoprecipitated with GFP-trap magnetic beads. The immunoprecipitate was analyzed by Western blotting using anti-GFP or anti-SKIP antibodies as indicated on the left.

(Co-IP) assay (Figure 4E). These results suggest that SKIP and STM function in the same complex to control SAM formation in Arabidopsis.

Consistent with the interaction between SKIP and STM, the mutation of SKIP and STM produced similar phenotypes in Arabidopsis. Both *skip-2* and *stm-1* plants exhibited severe defects in cell organization in the SAM, a lack of SAM formation at the shoot tip, failed production of normal leaves and shoots, and an inability to complete their life cycle (Figure 5, A and B). Thus, both SKIP and STM are required for SAM formation in Arabidopsis.

SKIP expression in the SAM is required for SAM formation and maintenance

SKIP is expressed constitutively during the plant life cycle (Wang et al., 2012). To assess the function of SKIP in the SAM, we specifically expressed SKIP in the SAM region by expressing *GFP-SKIP* driven by the native *STM* promoter (*pSTM::GFP-SKIP*) in *skip-2* plants. We first tested the specific expression of the native *STM* promoter in Arabidopsis (Wang et al., 2012; Landrein et al., 2015). Both *pSTM::STM-VENUS* and *pSTM::GFP-SKIP* were specifically expressed in the SAM region in embryos, while *pSKIP::SKIP-GFP* was expressed in whole embryos (Supplemental Figure S5), indicating that both promoters functioned as expected. We subsequently found that SKIP expression completely rescued the defects in cell organization and SAM formation observed in the *skip-2* mutant (Figure 6, A–D). In addition, SKIP expression in the SAM region in *skip-2* completely complemented SAM-mediated postembryonic development, including leaf, shoot, and floral organ production (Supplemental Figure S6, A–C). These results suggest that the expression of SKIP in the SAM region is required for SAM formation and development in Arabidopsis.

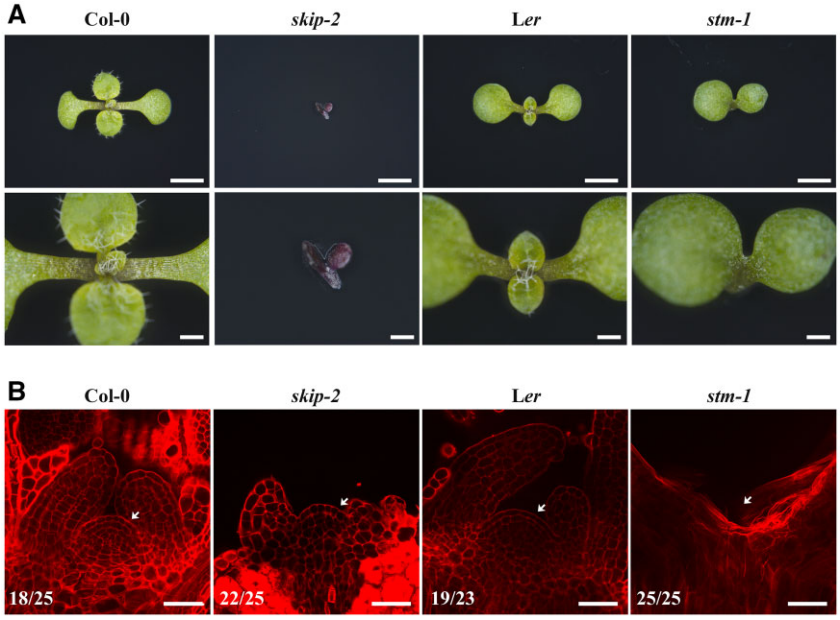

Figure 5 Both *skip-2* and *stm-1* exhibited defects in SAM development. A, Dissecting microscope images of the shoot apices of 9-day-old wild-type (Col-0), *skip-2* (Col-0), wild-type (*Ler*), and *stm-1* (*Ler*) plants from the top view. Scale bars: 2 mm (first) and 500 μm (second). B, Laser scanning confocal microscope observations of the SAM following mPS-PI staining. Scale bar: 40 μm. Arrows indicate the SAM. Numbers indicate the number of plants that exhibited a similar pattern out of the total number of plants observed.

To confirm this observation, we specifically knocked out SKIP in the SAM region by expressing *Cas9-SKIP-sgRNA* driven by the native *STM* promoter (Landrein et al., 2015) (*pSTM::Cas9-SKIP-sgRNA*) in a *skip-2* complementation line (*pSKIP::SKIP-GFP/skip-2*) (Figure 7A). We subsequently found that *Cas9-SKIP-sgRNA* expression in the SAM region did not confer SAM formation in our transgenic plants (Figure 7B). DNA sequence analysis indicated that *SKIP* had been edited to produce two new forms as the result of a frameshift that was predicted to generate very short truncated proteins (Figure 7C and Supplemental Figure S7, A–C). Among 349 individual, independent T1 transgenic lines, 155 exhibited SAM defects as indicated in Figure 7B. Among 65 independent T1 transgenic lines with a normal SAM, none of them possessed an edited form of *SKIP*, while among 124 independent T1 transgenic lines that exhibited a defect in the SAM, 102 exhibited *SKIP* editing as indicated (Figure 7C and Supplemental Figure S7, A–C). Further analysis revealed that SKIP-GFP was expressed in the SAM region with the same regular cellular organization observed in our *pSKIP::SKIP-GFP/skip-2* line; in contrast, no SKIP-GFP signal was observed in the SAM region of the *pSTM::Cas9-SKIP-sgRNA/pSKIP::SKIP-GFP/skip-2* transgenic lines, and the cellular organization in the SAM of our transgenic *pSTM::Cas9-SKIP-sgRNA* lines was irregular, similar to *skip-2* and *stm-1* (Figures 5, A and B and 7D). In addition, similar to *stm-1*, transgenic *pSTM::Cas9-SKIP-sgRNA* lines produced a few adventitious leaves from the apex at later developmental stages (Supplemental Figure S8, A and B). These findings suggest that the expression of SKIP in the SAM region is necessary for SAM formation in Arabidopsis.

The SKIP-STM complex works as a transcriptional activator to regulate the expression of target genes

STM localizes to both the nucleus and cytosol (Hay and Tsiantis, 2010). The translocation of STM from the nucleus to the cytosol, which is mediated by STM-interacting proteins, is one point of regulation in the function of STM (Hay and Tsiantis, 2010). In comparison, SKIP contains two nuclear localization sequences (NLSs) in its SNW and C-terminal domains, respectively, and it is a nuclear protein in Arabidopsis (Wang et al., 2012; Li et al., 2016). Therefore, SKIP may function as an STM-interacting protein to recruit STM to the nucleus, and the defects in SAM formation observed in *skip-2* may be due to the exclusion of STM from the nucleus caused by a loss of SKIP function. If this were the case, nuclear expression of STM would recue the SAM defects observed in *skip-2*. To test this, we fused 2 NLSs to the C-terminus of STM and GFP, in frame, after the NLSs to generate a nonmobile nuclear-localized version of STM (STM-2NLS-GFP) (Balkunde et al., 2017), which was expressed in *skip-2* plants under the control of the native *STM* promoter. Consistent with previous reports, overexpression of STM in wild-type plants produced a lobed leaf phenotype (Supplemental Figure S9A; Cole et al, 2006; Balkunde et al., 2017), indicating that STM-2NLS-GFP was functional in Arabidopsis under our conditions (Supplemental Figure S9A). However, although STM-2NLS-GFP was expressed and localized to the nucleus in *skip-2* plants based on the observation of overlapping STM-2NLS-GFP and DAPI signals, the nucleus-specific expression of STM in *skip-2* had no effect on SAM formation (Supplemental Figure S9, A and B). These results suggest that the defects in SAM formation in *skip-2* were not caused

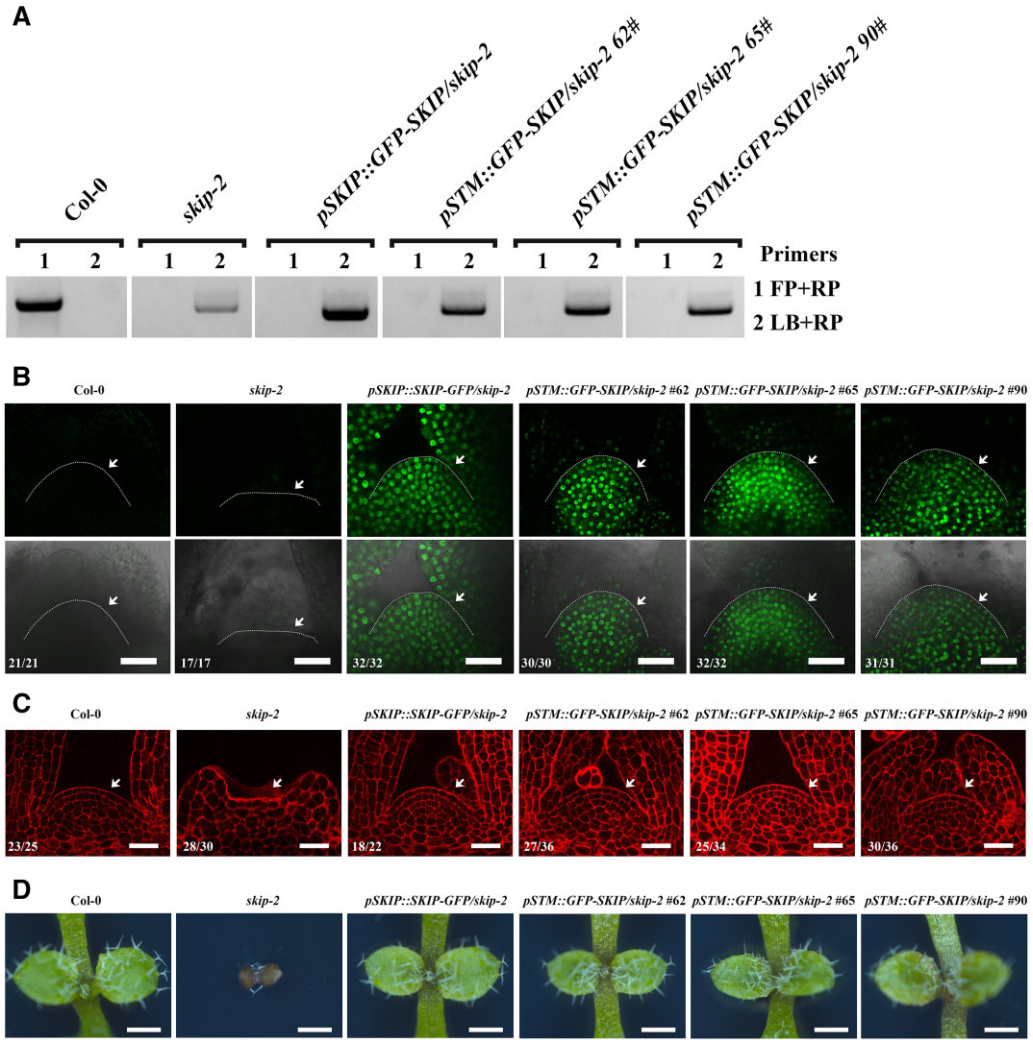

Figure 6 SKIP expression in the SAM region complemented the defect in SAM formation in *skip-2*. A, Genotyping of complemented *skip-2* transgenic plants by the transformation of *pSTM::GFP-SKIP* into *skip-2*. FP is forward primer; RP is reverse primer; LB is primer in T-DNA. B, Laser scanning confocal microscope images of the SAM in 9-day-old plants using the GFP channel (top) and "Merge" (bright-field + GFP) channel (bottom). Scale bar: 30 μm. Arrowheads indicate the SAM. C, Laser scanning confocal microscope observations of the SAM in 7-day-old plants following mPS-PI staining. Scale bar: 30 μm. Arrowheads indicate the SAM. The numbers in (B) and (C) indicate the number of plants that exhibited a similar pattern out of the total number of plants observed. D, Dissecting microscope images of the shoot apices of 7-day-old plants. Scale bar: 500 μm.

by a defect in the nuclear localization of STM due to the lack of its interacting partner, SKIP. Our results also suggest that both STM and SKIP are required for SAM formation in Arabidopsis.

STM works as a transcription factor to activate or repress the expression of specific target genes in plants (Sakamoto et al., 2001; Tsuda et al., 2014), while SKIP functions as a transcriptional coregulator of gene expression in Arabidopsis (Cao et al., 2015; Li et al., 2019). Therefore, the STM-SKIP complex may function as a transcriptional complex to regulate the expression of target genes in the SAM. *STM* (Tsuda et al., 2011), *KNAT1* (Tsuda et al., 2011), *CLV3* (Su et al., 2020), and *GA 2-oxidase 1* (*GA2OX1*) (Bolduc and Hake, 2009) are typical STM target genes. Therefore, the STM-SKIP complex may bind to chromatin where these genes reside and regulate their expression. Chromatin immunoprecipitation (ChIP) revealed that both STM and SKIP could bind directly to the promoter regions of *STM*, *KNAT1*, *CLAVATA 3* (*CLV3*), and *GA2OX1* (Figure 8A), and reverse transcription-quantitative real time polymerase chain reaction (RT-qPCR) analysis confirmed that the mutation of SKIP or STM decreased the expression of *STM*, *KNAT1*, *CLV3*, and *GA2OX1* in Arabidopsis (Figure 8B and Supplemental Figure S10). Thus, STM and SKIP regulate a similar set of target genes that are required for SAM formation. This supports the notion that a SKIP-STM transcriptional complex is required to regulate the expression of genes that support SAM formation in Arabidopsis.

Paf1c is required for SAM formation

Our previous results indicated that SKIP interacted with Paf1c, and SKIP-Paf1c-mediated *FLC* transcription is required for the regulation of floral transition in Arabidopsis (Cao et al., 2015; Li et al., 2019). In this work, it was observed that

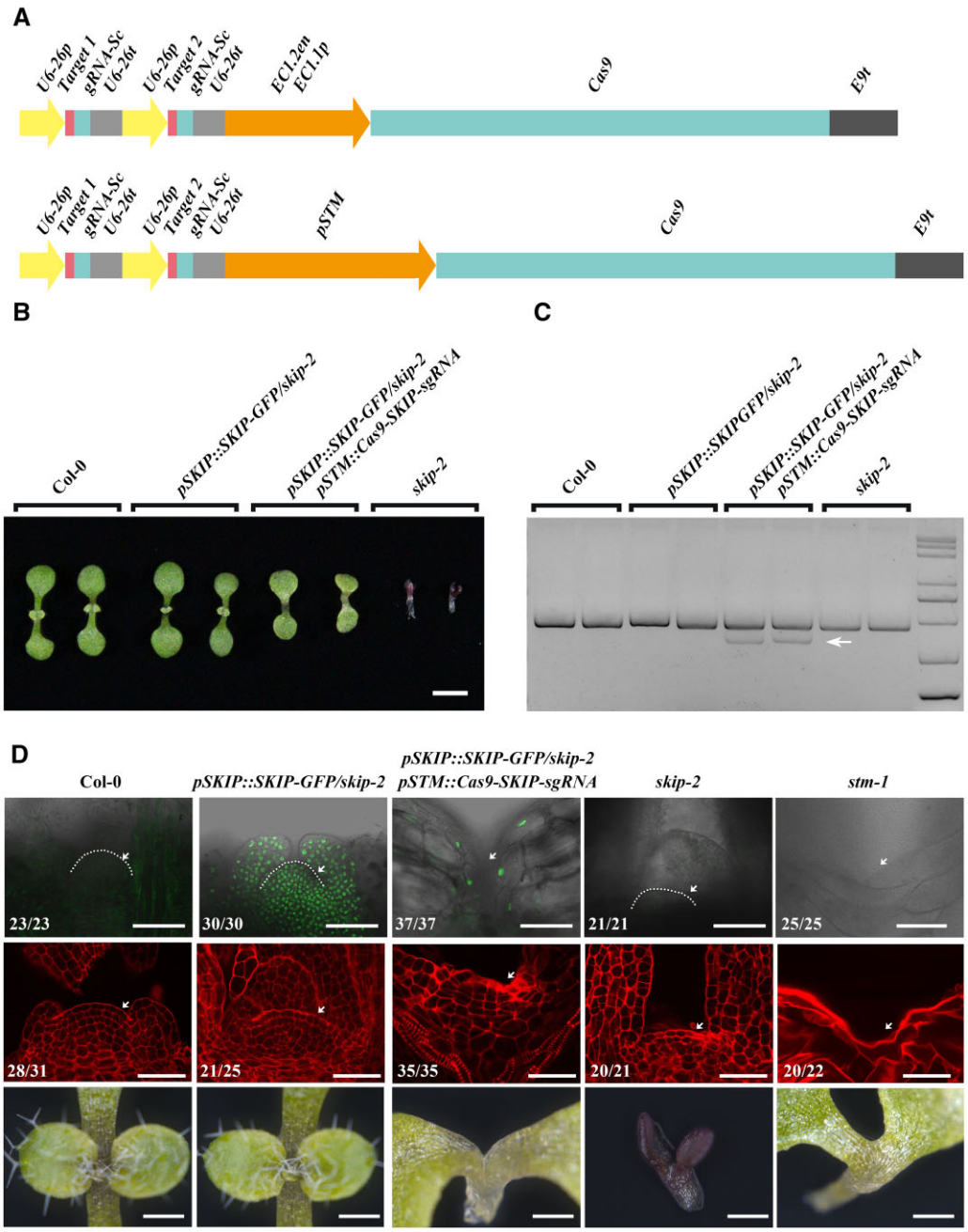

Figure 7 The knockout of *SKIP* in the SAM using *pSTM::Cas9-SKIP-sgRNA* caused a defect in SAM formation in Arabidopsis. A, Schematic diagram of the CRISPR/Cas9 binary vectors. The *Cas9* cassette was driven by the *EC1.1* (top) or *STM* (bottom) promoter, while *target-gRNA* was driven by the *U6-26* promoter. B, Phenotype of T1 transgenic *pSTM::Cas9-SKIP-sgRNA pSKIP::SKIP-GFP/skip-2* plants. Seven-day-old wild-type, *pSKIP::SKIP-GFP/skip-2*, *pSTM::Cas9-SKIP-sgRNA pSKIP::SKIP-GFP/skip-2*, and *skip-2* plants are shown. Scale bar: 2 mm. C, Genotype analysis of *SKIP* genomic DNA from T1 plants using the primer pair SKIPg1/2-F/R. The arrowhead indicates the edited *SKIP* genomic DNA, which lacked sequences between Target 1 and Target 2. D, In contrast to wild-type and *pSKIP::SKIP-GFP/skip-2* plants, the *pSTM::Cas9-SKIP-sgRNA pSKIP::SKIP-GFP/skip-2* plants exhibited a defect in SAM (arrowheads) formation. Laser scanning confocal microscope images of the SAM in 9-day-old plants using the GFP channel (top). Scale bar: 60 μm. Laser scanning confocal microscope observations of the SAM following mPS-PI staining (middle). Scale bar: 40 μm. Dissecting microscope images of the shoot apices of 7-day-old plants (bottom). Scale bar: 500 μm. Numbers indicate the number of plants that exhibited a similar pattern out of the total number of plants observed.

SKIP interacted with STM to regulate SAM development. Therefore, it is interesting to know whether Paf1c is required for SAM development. It was observed that EARLY FLOWERING 7 (*elf7*) exhibits similar SAM defects to *skip-1* and *stm-bum1* (Figure 9, A and B). FRET assay verified that STM interacts with ELF7 in *N. benthamiana* cells (Figure 9, C and D), and mutation in ELF7 or ELF8 down-regulated the expression of *KNAT1* and *GA2OX1* (Figure 9E). Those results

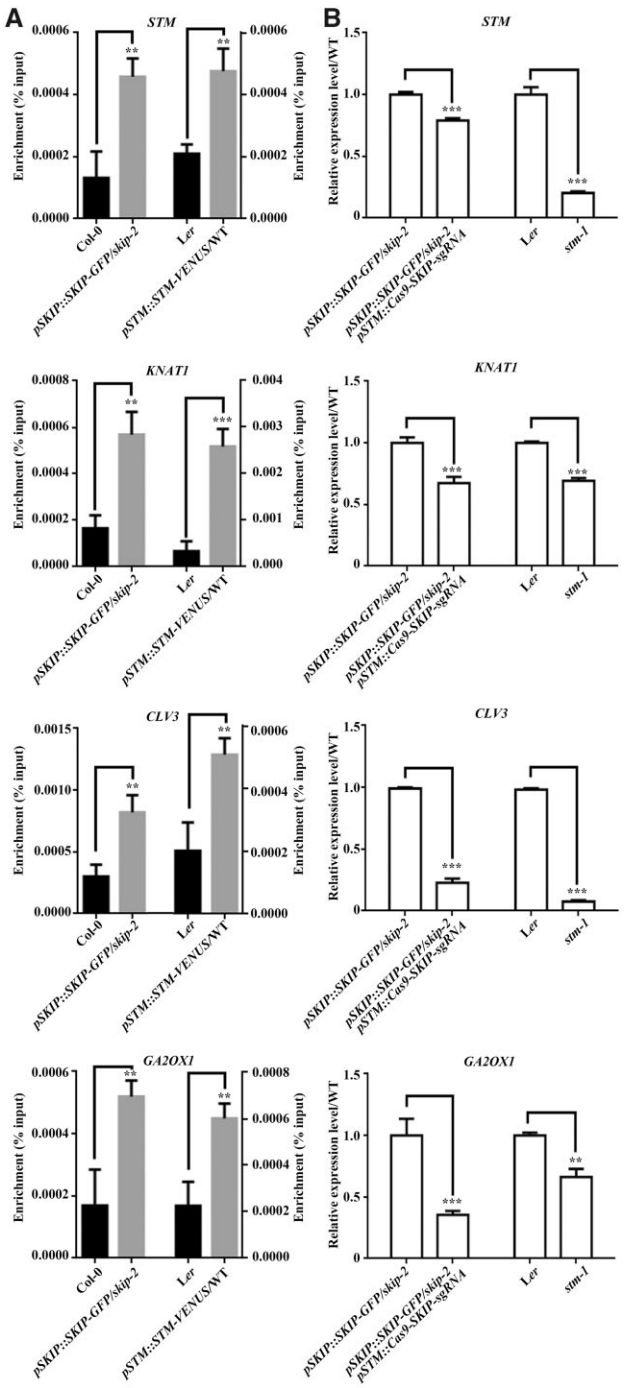

Figure 8 SKIP and STM bind to the promoter of target genes to regulate their expression in Arabidopsis. A, ChIP-qPCR of *STM* (first intron region), *KNAT1* (promoter region), *CLV3* (promoter region), and *GA2OX1* (promoter region). ChIP products were obtained by immunoprecipitation using samples from inflorescences containing only unopened flowers of wild-type (Col-0) and *pSKIP::SKIP-GFP/skip-2* (for SKIP binding) or wild-type (*Ler*) and *pSTM::STM-VENUS* (for STM binding) plants with anti-GFP antibodies. B, Relative expression levels of *STM*, *KNAT1*, *CLV3*, and *GA2OX1* as determined by RT-qPCR. The samples are from *pSKIP::SKIP-GFP/skip-2* and *pSTM::Cas9-SKIP-sgRNA pSKIP::SKIP-GFP/skip-2* (for SKIP-regulated expression) or *Ler* and *stm-1* (for STM-regulated expression) plants. The primers used are shown in Supplemental Table S1. The data represent the mean ± SD from three biological replicates. $^{**}P < 0.01$, $^{***}P < 0.001$ (Student's *t* test).

are consistent with the observation of the interaction between SKIP and Paf1c, and indicated that Paf1c is required for SAM formation.

Discussion

STM is a transcription factor that works with SKIP to regulate the expression of genes required for SAM formation and maintenance

SKIP is required for the expression of several genes, including *STM*, *KNAT1*, *CLV3*, *GA2OX1* (Figure 8, A and B), and *FLC* (Cao et al., 2015; Li et al., 2019). It also interacts with such transcriptional machinery as Paf1c (Cao et al., 2015; Li et al., 2019). However, neither SKIP nor Paf1c has a DNA-binding domain, so they are not capable of binding directly to target genes. Therefore, SKIP requires partner proteins for target selection. Transcription factors target specific genes by binding directly to those genes using their DNA-binding domain. Thus, transcription factors are good candidate partners for SKIP. We found that both SKIP and STM are required for SAM formation and maintenance (Figures 1–3 and 5–8), that SKIP interacts physically with STM in planta (Figure 4 and Supplemental Figure S3), and that SKIP binds to the promoter of STM target genes (Figure 8A). Thus, the transcription factor STM mediates target gene selection in SKIP-mediated SAM formation and maintenance by interacting with SKIP to regulate target gene expression. Therefore, SKIP may regulate distinct developmental processes by interacting with different transcription factors. As SKIP is also a splicing factor required for alternative gene splicing, it would be interesting to know whether SKIP couples the transcription and alternative splicing of its target genes and their transcripts.

SKIP is a cofactor of STM that regulates the expression of genes required for SAM formation and maintenance

STM is a transcription factor that regulates the expression of genes required for SAM formation and maintenance. To achieve this function, STM must work with cofactors to form a transcriptional complex (Hay and Tsiantis, 2010). BELL family proteins are cofactors of STM; STM and BELL proteins form heterodimers to regulate target genes (Cole et al., 2006), and different combinations of KNOX/BELL transcription factors may regulate different downstream genes. Within a STM–BELL heterodimer, STM is responsible for transcriptional activation while BELL is responsible for DNA binding (Cao et al., 2020). Another STM cofactor is mini-KNOX, a KNOX protein that lacks a homeodomain. Mini-KNOX interacts selectively with BELL proteins and affects their availability to form active STM-BELL complexes; therefore, mini-KNOX antagonizes the regulatory activity of STM-BELL complexes (Kimura et al., 2008; Magnani and Hake, 2008). These results indicate that KNOX proteins regulate target genes differently depending on their cofactor.

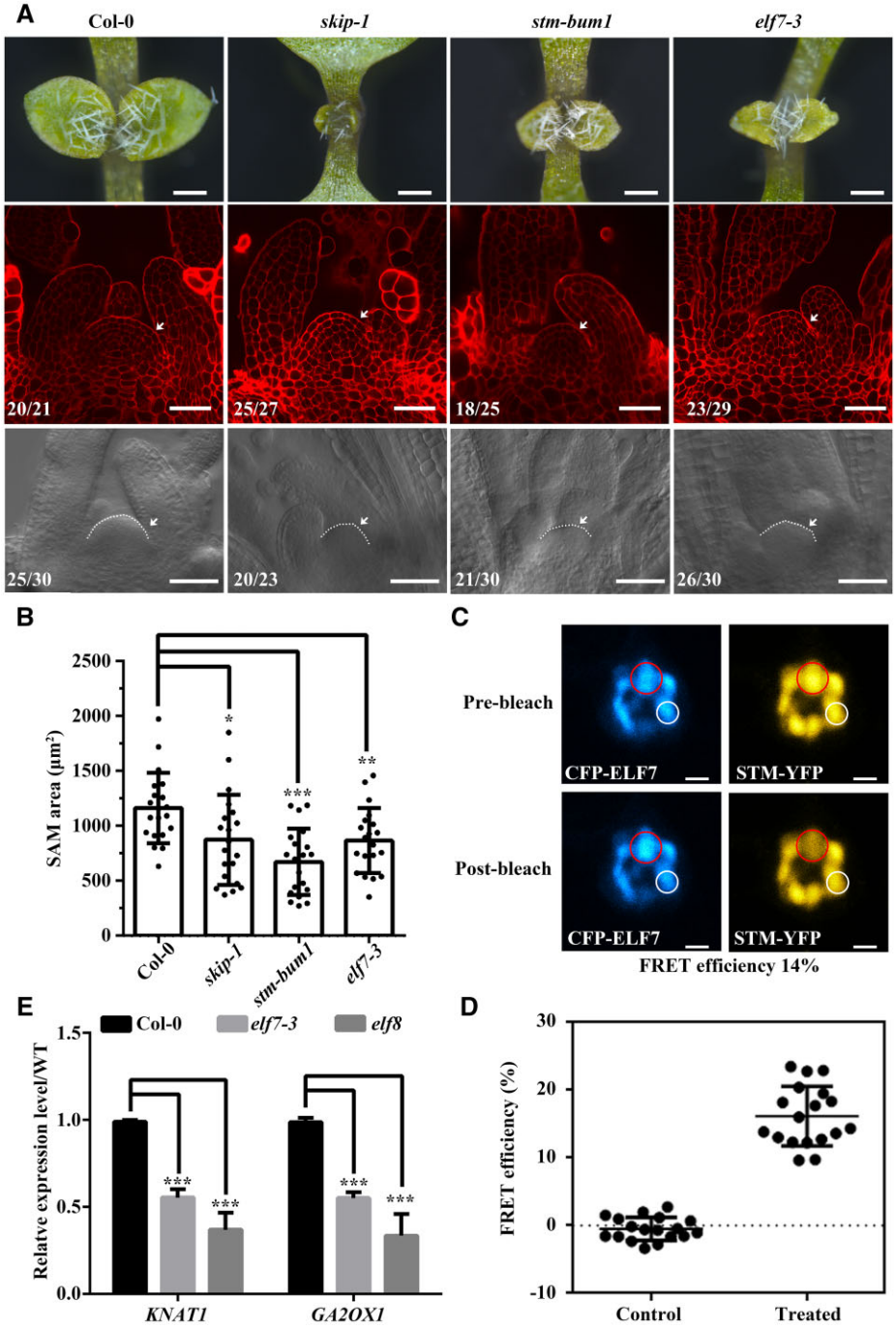

Figure 9 The mutation in ELF7 confers SAM defects in Arabidopsis. *elf7-3* exhibited similar SAM defects in Arabidopsis. A, Dissecting microscope images of the shoot apices of 7-day-old plants (top, scale bar: 400 μm). Laser scanning confocal microscope observations of the SAM following mPS-PI staining (middle, scale bar: 40 μm). Differential interference contrast microscopy images of the SAM (bottom, scale bar: 40 μm). Numbers indicate the number of plants that exhibited a similar pattern out of the total number of plants observed. White dashed lines and arrows indicate the SAM. B, SAM area was measured from bottom of (A). The data represent the mean ± SD from 20 SAM. $^{*}P < 0.05$, $^{**}P < 0.01$, $^{***}P < 0.001$ (Student's *t* test). C, FRET assay in *N. benthamiana* cells. Laser scanning confocal microscope images from the CFP and YFP channels before and after STM-YFP photobleaching are shown. Efficiency of FRET = (post ID-pre ID)/post ID, where ID is the intensity of the donor (CFP). Scale bar: 2 μm. D, The FRET efficiency from individual cells of three independent biological replicates. The control data were calculated from the nuclear speckle marked with a white circle in (C). The treated data were calculated from the nuclear speckle marked with a red circle in (C). The data represent the mean ± SD from 18 cells. E, Relative expression levels of KNAT1 and GA2OX1 as determined by RT-qPCR. The samples are from Col-0, elf7, and elf8 plants. The primers used are shown in Supplemental Table S1. The data represent the mean ± SD from three biological replicates. $^{***}P < 0.001$ (Student's *t* test).

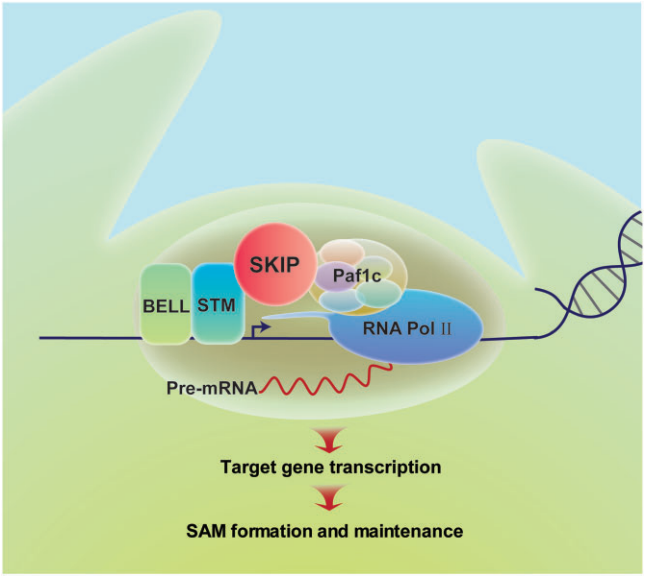

Figure 10 Proposed model for SKIP-STM-regulated gene expression and SAM formation in Arabidopsis. SKIP works as a cofactor with STM to recruit transcriptional machinery (e.g. Paf1c) to STM target genes. This promotes the initiation and elongation phases of transcription from these target genes, leading to formation and maintenance of the SAM in Arabidopsis.

In this study, we found that SKIP interacts with STM in a domain-friendly and flexible manner (Figure 4 and Supplemental Figure S3), and that both of them bind to the promoter of their target genes and are required for the expression of these genes (Figure 8, A and B). This suggests that SKIP is a cofactor of STM that helps promote its gene regulatory function. We previously confirmed that SKIP interacts with Paf1c to regulate the transcription of *FLC* (Cao et al, 2015; Li et al., 2019). Paf1c is a transcriptional mediator that is required for the initiation and elongation phases of transcription (Zhu et al., 2005; Cao et al., 2015). Interestingly, *VERNALIZATION INDEPENDENCE 3* (*VIP3*), which encodes a component of Paf1c, interacts genetically with *STM* (Takagi and Ueguchi, 2012), and the mutation of VIP3 confers a defect in PZ development, reducing the size of the SAM to half that in wild-type, and it produces a semi-dwarf phenotype in Arabidopsis (Fal et al., 2017). In this work, we also observed that mutation in ELF7, another component of Paf1c, confers similar SAM defects as that of STM and SKIP (Figure 9, A and B), and confirmed the physical interaction between STM and ELF7 (Figure 9, C and D). Taken together, these results suggest that SKIP functions as a cofactor of STM to recruit transcriptional machinery (e.g. Paf1c) to STM target genes and promote their transcription (i.e. initiation and elongation; Figure 10). However, as SKIP also works as a splicing factor and is required for the alternative splicing of pre-mRNAs in Arabidopsis (Wang et al., 2012; Feng et al., 2015; Li et al., 2019), mutation in *SKIP* has a slight defect in the splicing of *STM*, *KNAT1*, *CLV1*, and *CLV3* (but not obvious compared with that of a tolerance gene *PROTEIN S-ACYL TRANSFERASE 10* [*PAT10*]) (Supplemental Figure S11). Therefore, we cannot rule out the possibility that SKIP-mediated alternative splicing also contributes to the regulation of SAM development.

SKIP interacts with STM and possibly other KNOX family members required for the formation of axillary and floral meristems

There are four members of the KNOXI family in Arabidopsis (Hay and Tsiantis, 2010), and they exhibit identical yet distinct functions. For example, KNAT6 (but not KNAT2) acts redundantly with STM to regulate SAM activity and organ separation, while KNAT1 functions antagonistically with KNAT6 and KNAT2 in inflorescence development (Belles-Boix et al., 2006; Ragni et al., 2008). In addition, KNOX proteins are required for the formation of axillary and floral meristems (Roth et al., 2018; Cao et al., 2020). Considering that SKIP is a flexible protein (Supplemental Figure S3), it would be interesting to know whether SKIP interacts with KNOX family proteins other than STM, and whether SKIP is required for the formation of axillary and floral meristems to mediate branching and floral development in Arabidopsis.

Both SKIP and KNOX proteins are conserved among plants and possibly even among eukaryotes, and KNOX proteins function in diverse developmental contexts (Kimura et al., 2008; Hay and Tsiantis, 2010; Kierzkowski et al., 2019). It will thus be interesting to determine whether our model for SKIP-KNOX function in Arabidopsis applies to diverse species and in distinct developmental contexts.

Materials and methods

Plant materials and growth conditions

All Arabidopsis (*A. thaliana*) plant materials used in this study were of the Columbia-0 (Col-0) or Landsberg *erecta* (*Ler*) ecotype. The following mutants were described previously: *skip-1* (Col-0) (Wang et al., 2012), *skip-2* (Col-0) (Li et al., 2016), *stm-1* (*Ler*) (Long et al., 1996), and *STM-VENUS*/WT (*Ler*) (Heisler et al., 2005; Shi et al., 2016), *stm-bum1* (Col-0) (Shi et al., 2016), and *elf7-3* (Col-0) (Cao et al., 2015). All mutations were confirmed by PCR and sequencing. The primers used to characterize the mutants by PCR are given in Supplemental Table S1. Seedlings were grown in a Percival CU36L5 growth chamber (Percival Scientific, Perry, IA, USA) under 16 h of white light at an intensity of 70 mmol m^{-2} s^{-1} at 22°C, followed by 8 h of darkness at 18°C. Adult plants were cultivated in a greenhouse and grown at 22°C for 16 h in the light at a white light intensity of 150 mmol m^{-2} s^{-1} and at 18°C for 8 h in the dark.

Construction of transgenic plants

For *pSKIP::SKIP* construction, the *pSKIP::SKIP* genomic region (1,800-bp promoter region and whole coding region) was amplified from Col-0 genomic DNA then cloned into *Pst* I and *Sac* I sites of the binary vector pCAMBIA1300 containing the NOS terminator. For *pSTM::GFP-SKIP* construction,

the *SKIP* genomic region fused to *GFP* driven by the native *STM* promoter (Landrein et al., 2015) was cloned into *Pst* I and *Sac* I sites of the binary vector pCAMBIA1300 containing the NOS terminator. For *pSTM::Cas9-SKIP-sgRNA* construction, the *SKIP-sgRNA* cassette was obtained by PCR amplification from pCBC-DT1T2 using the primer pair DT1-F0/BsF and DT2-R0/BsR. The PCR products were digested with *Bsa* I and the digested fragment was inserted into pHEE401 (Wang et al., 2015), resulting in the production of *Cas9-SKIP-sgRNA*. The *STM* promoter was inserted into the *Spe* I and *Xba* I sites of pHEE401, resulting in the production of *pSTM::Cas9-SKIP-sgRNA*. For *pSTM::STM-2NLS-GFP* construction, the *STM* genomic region fused to the *2NLS-GFP* tag driven by its native promoter was cloned into *Pst* I and *Sac* I sites of the binary vector pCAMBIA1300 containing the NOS terminator. For *pSKIP::SKIP-CERULEAN* construction, the *SKIP* genomic region fused to the *CERULEAN* tag driven by its native promoter was cloned into the *Pst* I and *Sac* I sites of binary vector pCAMBIA1300 containing the NOS terminator. For *pSKIP::SKIP-GFP* construction, the *SKIP* genomic region fused to the *GFP* tag driven by its native promoter was cloned into the *Pst* I and *Sac* I sites of binary vector pCAMBIA1300 containing the NOS terminator. The primers and restriction sites used to construct for expression vector are given in Supplemental Table S1.

Yeast two-hybrid assays

The coding regions of *SKIP* and various *SKIP* deletion derivatives were cloned into pGADT7, while the coding region of *STM* was cloned into pGBKT7. Different combinations of vectors were cotransformed into *Saccharomyces cerevisiae* strain AH109. The primers and restriction sites used to clone the coding sequences of *SKIP* and *STM* are included in Supplemental Table S1. Transformation, yeast growth, and protein extraction were performed as described in the Clontech Yeast Protocols Handbook.

FRET assays

FRET assays were conducted as described previously (Li et al., 2016). The coding regions of *SKIP* and *STM* were fused to *GFP* and *RFP*, or the coding regions of *ELF7* and *STM* were fused to *CFP* and *YFP*, respectively, and then cloned into the binary vector pCAMBIA1300. The primers used to clone the coding sequences of *SKIP* and *STM* are included in Supplemental Table S1. The two constructs were transiently expressed in *N. benthamiana* leaves infiltrated with *Agrobacterium tumefaciens* strains carrying the appropriate binary plasmids.

Two days after transformation, a FRET assay was performed with a Zeiss 780 laser scanning confocal microscope (Jena, Germany). Prebleached images of the donor (GFP/CFP) and acceptor (RFP/YFP) were acquired using the GFP/CFP channel and RFP/YFP channel. Next, the fluorescence intensity in a region of interest in the nucleus was recorded using the software provided by the manufacturer (Zeiss, Jena, Germany). STM-RFP/STM-YFP was then photobleached by repeated scanning of the selected region with a 561-/514-nm laser beam. Postbleached images of GFP-SKIP/CFP-ELF7 and STM-RFP/STM-YFP were acquired after the photobleaching of RFP/YFP, respectively. After correcting for changes in image registration, the fluorescence intensities of the two GFP images were calculated. The energy transfer efficiency between the two interacting proteins was calculated as follows: Efficiency of FRET = (post ID-pre ID)/post ID, where ID is the intensity of the donor (GFP/CFP). The experimental setup used for the confocal work is given in Supplemental Table S2.

Co-IP

Inflorescences containing only unopened flowers in a *Ler* or *pSTM::STM-Venus* background were dissected for immunoprecipitation. Total protein was extracted with immunoprecipitation buffer (50 mM Tris–HCl, pH 8.0, 150 mM NaCl, 0.3% [v/v] NP40, 10% [v/v] glycerol, 1 mM PMSF, and protease inhibitor] and immunoprecipitated with GFP-Trap magnetic beads. The immunoprecipitates were separated by sodium dodecyl sulfate-polyacrylamide gel electrophoresis and analyzed by Western blotting with anti-GFP or anti-SKIP antibodies.

Histology and microscopy

Each specimen was prepared as described previously (Lee et al., 2010). To prepare semi-thin sections, shoot tips were fixed in a solution containing 2.5% (v/v) glutaraldehyde in 0.1 M PBS buffer (pH 7.2) under vacuum conditions for 30 min. After fixing for 2 days at 4°C, the shoot tips were rinsed twice with phosphate buffer and then dehydrated at room temperature in a graded series of ethanol starting at 30% then going to 40%, 50%, 60%, 70%, 80%, 90%, 95%, and 100% (v/v). The specimens were embedded in Spurr's low-viscosity embedding medium. Infiltration was started in a 2:1 ethanol/embedding medium. The specimens were left in the mixture with swirling of the container for 2 h after which the medium was replaced with a 1:1 ethanol/embedding medium and left in the container, which was swirled, for 4 h. Next, the medium was replaced with 1:3 ethanol/embedding medium and incubated with swirling of the container for another 6 h. After that, the mixture was drained and embedding medium was added to the container and left overnight. After curing the specimens for 48 h at 65°C, the specimens were mounted and sectioned at a thickness of 1 μm using a UC6 microtome (Leica, Wetzlar, Germany). After staining briefly with 0.1% toluidine blue, the sections were observed under bright-field optics using an Axio Imager M2 microscope (Zeiss).

Modified pseudo-Schiff propidium iodide staining

Each specimen was prepared as described previously (Truernit et al., 2008) with some modifications. For modified pseudo-Schiff propidium iodide (mPS-PI) staining, shoot tips were fixed in 50% (v/v) methanol and 10% (v/v) acetic acid overnight at 4°C then washed with water and dehydrated in an ethanol series (30%, 50%, 70%, 80%, 90%, 95%, and 100% [v/v]). The shoot tips were partially rehydrated through a

graded ethanol series from 100% to 15% (v/v). The shoot tips were then rinsed with water and then treated with 1% (w/v) periodic acid for 40 min at room temperature. The shoot tips were then rinsed with water again and incubated in Schiff reagent (0.2 g of $NaHSO_3$, 200 μg of PI, 62.5 μL of HCl, and 9.8 mL of ddH_2O) for 2 h. The shoot tips were next covered with chloral hydrate solution (8 g of chloral hydrate, 2 mL of glycerol, and 4 mL of ddH_2O) for 10 min and mounted in Hoyer's solution (30 g of gum arabic, 200 g of chloral hydrate, 20 g of glycerol, and 50 mL of water) on slides for observation. The size of each cleared shoot meristem was measured using the software provided by Zeiss for image analysis.

Image acquisition

An Axio Zoom V16 dissecting microscope (Zeiss) was used to photograph living seedlings. The mPS-PI-stained samples, CERULEAN signal, and VENUS signal in vivo were observed with a Zeiss 780 laser scanning confocal microscope. The DAPI-stained samples and GFP signal in vivo were imaged with a Leica SP8 X confocal microscope (Wetzlar, Germany). The experimental setup used for the confocal work is given in Supplemental Table S2.

Tissues clearing and SAM observation

Each specimen was prepared as described previously (Su et al., 2020) with some modifications. Shoot tips were fixed in 50% (v/v) methanol and 10% (v/v) acetic acid 3 h at room temperature. Then washed with water and dehydrated in an ethanol series (100%, 95%, 85%, and 70% [v/v]). Shoot tips were mounted in chloral hydrate solution (8 g of chloral hydrate, 2 mL of glycerol, and 4 mL of ddH_2O) for 3 h. Next, the cleared tissues with SAM were examined by differential interference contrast microscopy using an Axio Imager M2 microscope (Zeiss). The size of each cleared shoot meristem was measured using software provided by Zeiss for image analysis.

Collect samples at T1 generation from CRISPR lines

Enough T0 seeds were generated and more than 200 individual T1 seedlings were collected for the first replicate of DNA sequencing and RT-qPCR experiments, and >50 individual T1 seedlings for other two biological replicates of DNA sequencing and RT-qPCR experiments.

RNA extraction and RT-qPCR

Total RNA was isolated from 9-day-old wild-type or mutant seedlings using Trizol reagent (Invitrogen, Carlsbad, CA, USA) and then treated with RNase-free DNase I (Promega, Madison, WI, USA) to degrade remaining DNA. Next, 3 μg of total RNA was used for cDNA synthesis with a RevertAid First Strand cDNA Synthesis Kit with oligo(dT) primer (Thermo Fisher Scientific, Waltham, MA, USA). RT-qPCR was performed using the cDNA as a template; the primers are shown in Supplemental Table S1. Takara SYBR Premix Ex Taq (Takara Bio, Otsu, Japan) and a 7500 Real-Time PCR instrument (Applied Biosystems, Foster City, CA, USA) were used for RT-qPCR.

ChIP assays

ChIP was performed as described previously (Cheng et al., 2013) with some modifications. Inflorescences containing only unopened flowers from *pSKIP::SKIP-GFP/skip-2* and *pSTM::STM-Venus*/WT (*Ler*) plants were dissected and ground in liquid nitrogen. The powder was fixed in PBS buffer containing 1% (v/v) formaldehyde for 10 min at 4°C and the unreacted formaldehyde was quenched with glycine for 10 min. Following the isolation of nuclei and immunoprecipitation with anti-GFP antibodies, the DNA products were eluted with elution buffer. Quantitative PCR was performed using the bound DNA fragments as templates. The DNA samples underwent 45 cycles of amplification using the primers shown in Supplemental Table S1.

Statistical analysis

The statistical analysis in this study was conducted by two-sided unpaired *t* test.

Accession numbers

Sequence data from this article can be found in the GenBank/EMBL data libraries under the following accession numbers: SKIP, NM_001036214.3; STM, NM_104916.4; ELF7, NM_106622.5; KNAT1, NM_116884.4; CLV3, NM_128283.2; GA2OX1, NM_106491.2; WUS, NM_127349.4; PAT10, NM_114998.5.

Supplemental data

The following materials are available in the online version of this article.

Supplemental Figure S1. Characterization of the *skip-2* mutant.

Supplemental Figure S2. *skip-1* has a semi-dwarf phenotype.

Supplemental Figure S3. The interaction between STM and full-length or truncated SKIP as determined in yeast two-hybrid assays.

Supplemental Figure S4. The subcellular localization of STM and co-localization of SKIP and STM in Arabidopsis.

Supplemental Figure S5. *STM* promoter-driven expression of SKIP and STM in the SAM during early embryogenesis.

Supplemental Figure S6. SKIP expression in the SAM region complemented the life cycle defects observed in *skip-2*.

Supplemental Figure S7. *pSTM::Cas9-SKIP-sgRNA*-edited *SKIP* in Arabidopsis.

Supplemental Figure S8. The knockout of *SKIP* in the SAM using *pSTM::Cas9-SKIP-sgRNA* caused a defect in SAM at later developmental stages in Arabidopsis.

Supplemental Figure S9. The transformation of nuclear-localized STM in *skip-2* had no effect on SAM formation in *skip-2* plants.

Supplemental Figure S10. Mutation in *SKIP* down-regulated the expression of genes required for SAM development.

Supplemental Figure S11. The effect of SKIP mutation on the splicing of genes required for SAM development and salt tolerance.

Supplemental Table S1. The primers used in this study.

Supplemental Table S2. The experimental setup used for the confocal work in this study.

Acknowledgments

We thank Dr. Jessica Habashi for critical reading of the manuscript. We also thank Dr. Xianyong Sheng of the Imaging Center, College of life Sciences, Capital Normal University (Beijing, China), for performing the FRET and localization of proteins assays.

Funding

This work was supported by grants from the National Natural Science Foundation of China (31972857, 32000454).

Conflict of interest statement. None declared.

References

Balkunde R, Kitagawa M, Xu XM, Wang J, Jackson D (2017) SHOOT MERISTEMLESS trafficking controls axillary meristem formation, meristem size and organ boundaries in Arabidopsis. Plant J **90**: 435–446

Belles-Boix E, Hamant O, Witiak SM, Morin H, Traas J, Pautot V (2006) KNAT6: an Arabidopsis homeobox gene involved in meristem activity and organ separation. Plant Cell **18**: 1900–1907

Bolduc N, Hake S (2009) The maize transcription factor KNOTTED1 directly regulates the gibberellin catabolism gene *ga2ox1*. Plant Cell **21**: 1647–1658

Byrne ME, Barley R, Curtis M, Arroyo JM, Dunham M, Hudson A, Martienssen RA (2000) *Asymmetric leaves1* mediates leaf patterning and stem cell function in Arabidopsis. Nature **408**: 967–971

Cao X, Wang J, Xiong Y, Yang H, Yang M, Ye P, Bencivenga S, Sablowski R, Jiao Y (2020) A self-activation loop maintains meristematic cell fate for branching. Curr Biol **30**: 1893–1904

Cao Y, Ma LG (2019) To splice or to transcribe: SKIP-mediated environmental fitness and development in plants. Front Plant Sci **10**: 1222

Cao Y, Wen L, Wang Z, Ma LG (2015) SKIP interacts with the Paf1 complex to regulate flowering via the activation of *FLC* transcription in Arabidopsis. Mol Plant **8**: 1816–1819

Cheng ZJ, Wang L, Sun W, Zhang Y, Zhou C, Su YH, Li W, Sun TT, Zhao XY, Li XG, et al (2013) Pattern of auxin and cytokinin responses for shoot meristem induction results from the regulation of cytokinin biosynthesis by AUXIN RESPONSE FACTOR3. Plant Physiol **161**: 240–251

Chung Y, Zhu Y, Wu MF, Simonini S, Kuhn A, Armenta-Medina A, Jin R, Østergaard L, Gillmor CS, Wagner D (2019) Auxin response factors promote organogenesis by chromatin-mediated repression of the pluripotency gene *SHOOTMERISTEMLESS*. Nat Commun **10**: 886

Cole M, Nolte C, Werr W (2006) Nuclear import of the transcription factor SHOOT MERISTEMLESS depends on heterodimerization with BLH proteins expressed in discrete sub-domains of the shoot apical meristem of *Arabidopsis thaliana*. Nucleic Acids Res **34**: 1281–1292

Cui X, Zhang Z, Wang Y, Wu J, Han X, Gu X, Lu T (2019) TWI1 regulates cell-to-cell movement of OSH15 to control leaf cell fate. New Phytol **221**: 326–340

Dinneny JR, Benfey P (2008) Plant stem cell niches: standing the test of time. Cell **132**: 553–557

Fal K, Liu M, Duisembekova A, Refahi Y, Haswell ES, Hamant O (2017) Phyllotactic regularity requires the Paf1 complex in Arabidopsis. Development **144**: 4428–4436

Feng J, Li J, Gao Z, Lu Y, Yu J, Zheng Q, Yan S, Zhang W, He H, Ma LG, et al (2015) SKIP confers osmotic tolerance during salt stress by controlling alternative gene splicing in Arabidopsis. Mol Plant **8**: 1038–1052

Folk P, Puta F, Skruzny M (2004) Transcriptional coregulatory SNW/SKIP: the concealed tie of dissimilar pathways. Cell Mol Life Sci **61**: 629–640

Guo M, Thomas J, Collins G, Timmermans MC (2008) Direct repression of *KNOX* loci by the ASYMMETRIC LEAVES1 complex of Arabidopsis. Plant Cell **20**: 48–58

Hackbusch J, Richter K, Muller J, Salamini F, Uhrig JF (2005) A central role of *Arabidopsis thaliana* ovate family proteins in networking and subcellular localization of 3-aa loop extension homeodomain proteins. Proc Natl Acad Sci USA **102**: 4908–4912

Hake S, Smith HMS, Holtan H, Magnani E, Mele G, Ramirez J (2004) The role of *KNOX* genes in plant development. Annu Rev Cell Dev Biol **20**: 125–151

Hay A, Tsiantis M (2010) KNOX genes: versatile regulators of plant development and diversity. Development **137**: 3153–3165

Heisler MG, Ohno C, Das P, Sieber P, Reddy GV, Long JA, Meyerowitz EM (2005) Patterns of auxin transport and gene expression during primordium development revealed by live imaging of the Arabidopsis inflorescence meristem. Curr Biol **15**: 1899–1911

Jones MA, Williams BA, McNicol J, Simpson CG, Brown JW, Harmer SL (2012) Mutation of Arabidopsis spliceosomal timekeeper locus1 causes circadian clock defects. Plant Cell **24**: 4066–4082

Kierzkowski D, Runions A, Vuolo F, Strauss S, Lymbouridou R, Routier-Kierzkowska AL, Wilson-Sánchez D, Jenke H, Galinha C, Mosca G, et al. (2019) A growth-based framework for leaf shape development and diversity. Cell **177**: 1405–1418

Kimura S, Koenig D, Kang J, Yoong FY, Sinha N (2008) Natural variation in leaf morphology results from mutation of a novel KNOX gene. Curr Biol **18**: 672–677

Kumaran MK, Bowman JL, Sundaresan V (2002) YABBY polarity genes mediate the repression of KNOX homeobox genes in Arabidopsis. Plant Cell **14**: 2761–2770

Landrein B, Kiss A, Sassi M, Chauvet A, Das P, Cortizo M, Laufs P, Takeda S, Aida M, Traas J, et al (2015) Mechanical stress contributes to the expression of the STM homeobox gene in Arabidopsis shoot meristems. eLife **4**: e07811

Lee SY, Kim H, Hwang HJ, Jeong YM, Na SH, Woo JC, Kim SG (2010) Identification of tyrosyl-DNA phosphodiesterase as a novel DNA damage repair enzyme in Arabidopsis. Plant Physiol **154**: 1460–1469

Li Y, Yang J, Shang X, Lv W, Xia C, Wang C, Feng J, Cao Y, He H, Li L, et al (2019) SKIP regulates environmental fitness and floral transition, respectively, by forming two distinct complexes in Arabidopsis. New Phytol **224**: 321–335

Li Y, Xia C, Feng J, Yang D, Wu F, Cao Y, Li L, Ma LG (2016) The SNW domain of SKIP is required for its integration into the spliceosome and its interaction with the Paf1 complex in Arabidopsis. Mol Plant **9**: 1040–1050

Liu L, Li C, Song S, Teo ZWN, Shen L, Wang Y, Jackson D, Yu H (2018) FTIP-dependent STM trafficking regulates shoot meristem development in Arabidopsis. Cell Reports **23**: 1879–1890

Long JA, Barton MK (2000) Initiation of axillary and floral meristems in Arabidopsis. Dev Biol **218**: 341–353

Long JA, Moan EI, Medford JI, Barton MK (1996) A member of the KNOTTED class of homeodomain proteins encoded by the *STM* gene of Arabidopsis. Nature **379**: 66–69

Magnani E, Hake S (2008) KNOX lost the OX: the Arabidopsis KNATM gene defines a novel class of KNOX transcriptional regulators missing the homeodomain. Plant Cell **20**: 875–887

Németh K, Salchert K, Putnoky P, Bhalerao R, Koncz-Kálmán Z, Stankovic-Stangeland B, Bakó L, Mathur J, Okrész L, Stabel S, et al. (1998) Pleiotropic control of glucose and hormone responses by PRL1, a nuclear WD protein, in Arabidopsis. Genes Dev **12**: 3059–3073

Palma K, Zhao Q, Cheng YT, Bi D, Monaghan J, Cheng W, Zhang Y, Li X (2007) Regulation of plant innate immunity by three proteins in a complex conserved across the plant and animal kingdoms. Genes Dev **21**: 1484–1493

Ragni L, Belles-Boix E, Gunl M, Pautot V (2008) Interaction of KNAT6 and KNAT2 with BREVIPEDICELLUS and PENNYWISE in Arabidopsis inflorescences. Plant Cell **20**: 888–900

Roth O, Alvarez JP, Levy M, Bowman JL, Ori N, Shani E (2018) The KNOXI transcription factor SHOOT MERISTERMLESS regulates floral fate in Arabidopsis. Plant Cell **30**: 1309–1321

Rutjens B, Bao D, van Eck-Stouten E, Brand M, Smeekens S, Proveniers M (2009) Shoot apical meristem function in Arabidopsis requires the combined activities of three BEL1-like homeodomain proteins. Plant J **58**: 641–654

Sakamoto T, Kamiya N, Ueguchi-Tanaka M, Iwahori S, Matsuoka M (2001) KNOX homeodomain protein directly suppresses the expression of a gibberellin biosynthetic gene in the tobacco shoot apical meristem. Genes Dev **15**: 581–590

Shi B, Zhang C, Tian C, Wang J, Wang Q, Xu T, Xu Y, Ohno C, Sablowski R, Heisler MG, et al (2016) Two-step regulation of a meristematic cell population acting in shoot branching in Arabidopsis. PLoS Genet **12**: e1006168

Scheres B (2007) Stem-cell niches: nursery rhymes across kingdoms. Nat Rev Mol Cell Biol **8**: 345–354

Su YH, Zhou C, Li YJ, Yu Y, Tang LP, Zhang WJ, Yao WJ, Huang R, Laux T, Zhang XS (2020) Integration of pluripotency pathways regulates stem cell maintenance in the Arabidopsis shoot meristem. Proc Natl Acad Sci USA **117**: 22561–22571

Takagi N, Ueguchi C (2012) Enhancement of meristem formation by bouquet-1, a mis-sense allele of the vernalization independence 3 gene encoding a WD40 repeat protein in *Arabidopsis thaliana*. Genes Cells Devoted Mol Cell Mech **17**: 982–993

Truernit E, Bauby H, Dubreucq B, Grandjean O, Runions J, Barthelemy J, Palauqui JC (2008) High-resolution whole-mount imaging of three-dimensional tissue organization and gene expression enables the study of phloem development and structure in Arabidopsis. Plant Cell **20**: 1494–1503

Tsuda K, Hake S (2015) Diverse functions of KNOX transcription factors in the diploid body plan of plants. Curr Opin Plant Biol **27**: 91–96

Tsuda K, Ito Y, Sato Y, Kurata N (2011) Positive autoregulation of a KNOX gene is essential for shoot apical meristem maintenance in rice. Plant Cell **23**: 4368–4381

Tsuda K, Kurata N, Ohyanagi H, Hake S (2014) Genome-wide study of KNOX regulatory network reveals brassinosteroid catabolic genes important for shoot meristem function in rice. Plant Cell **26**: 3488–3500

Wahl MC, Cindy L, Will CL, Lührmann R (2009) The spliceosome: design principles of a dynamic RNP machine. Cell **136**: 701–718

Wan R, Bai R, Zhan X, Shi Y (2020) How is precursor messenger RNA spliced by the spliceosome? Annu Rev Biochem **89**: 333–358

Wang X, Wu F, Xie Q, Wang H, Wang Y, Yue Y, Gahura O, Ma S, Liu L, Cao Y, et al (2012) SKIP is a component of the spliceosome linking alternative splicing and the circadian clock in Arabidopsis. Plant Cell **24**: 3278–3295

Wang ZP, Xing HL, Dong L, Zhang HY, Han CY, Wang XC, Chen QJ (2015) Egg cell-specific promoter-controlled CRISPR/Cas9 efficiently generates homozygous mutants for multiple target genes in Arabidopsis in a single generation. Genome Biol **16**: 144

Weigel D, Jurgens G (2002) Stem cells that make stems. Nature **415**: 751–754

Williams LE (2021) Genetics of shoot meristem and shoot regeneration. Annu Rev Genet **55**: 661–681

Winter N, Kollwig G, Zhang S, Kragler F (2007) MPB2C, a microtubule -associated protein, regulates non-cell-autonomy of the homeodomain protein KNOTTED1. Plant Cell **19**: 3001–3018

Xu L, Shen WH (2008) Polycomb silencing of KNOX genes confines shoot stem cell niches in Arabidopsis. Curr Biol **18**: 1966–1971

Xu XM, Wang J, Xuan Z, Goldshmidt A, Borrill PGM, Hariharan N, Kim JY, Jackson D (2011) Chaperonins facilitate KNOTTED1 cell-to-cell trafficking and stem cell function. Science **333**: 1141–1144

Zhang C, Wang J, Wenkel S, Chandler JW, Werr W, Jiao Y (2018) Spatiotemporal control of axillary meristem formation by interacting transcriptional regulators. Development **145**: dev158352

Zhu B, Zheng Y, Pham AD, Mandal SS, Erdjument-Bromage H, Tempst P, Reinberg D (2005) Monoubiquitination of human histone H2B: the factors involved and their roles in HOX gene regulation. Mol Cell **20**: 601–611